Magn Reson Med Sci 2018; 17; 203–210
doi:10.2463/mrms.mp.2017-0024
Published Online: December 7, 2017

MAJOR PAPER

The Value of Lesion Size as an Adjunct to the BI-RADS-MRI 2013 Descriptors in the Diagnosis of Solitary Breast Masses

Makiko Kawai[1], Masako Kataoka[1*], Shotaro Kanao[1], Mami Iima[1], Natsuko Onishi[1], Akane Ohashi[1], Rena Sakaguchi[1], Masakazu Toi[2], and Kaori Togashi[1]

Purpose: This study aimed to evaluate the MRI findings of breast solitary masses in diagnostic procedures to decide the appropriate category based on American College of Radiology (ACR) BI-RADS-MRI 2013, with the focus on lesion size.

Methods: A retrospective review of 2,603 consecutive breast MRI reports identified 250 pathologically-proven solitary breast masses. Dynamic-contrast enhanced images and diffusion-weighted images were performed on a 3.0/1.5 Tesla Scanner with a 16/4 channel dedicated breast coil. MRI findings were re-evaluated according to ACR BI-RADS-MRI 2013. BI-RADS-MRI descriptors, lesion size and minimum apparent diffusion coefficient (ADC) value were statistically analyzed using univariate/multivariate logistic regression analysis and receiver operator characteristic (ROC) analysis. Based on the results, a diagnostic decision tree was constructed.

Results: Of the 250 lesions, 152 (61%) were malignant and 98 (39%) were benign. In univariate logistic regression analysis, most of the BI-RADS descriptors, lesion size, and ADC value were significant. Lesion size and ADC value were binarized with optimal cut-off values of 12 mm and 1.1×10^{-3} mm^2/s, respectively. Multivariate logistic regression analysis showed that lesion size (≥12 mm or not), margin (circumscribed or not), kinetics (washout or not) and internal enhancement characteristics (IEC) (rim enhancement present or absent) significantly contributed to the diagnosis ($P < 0.05$). Using these four significant parameters, a decision tree was constructed to categorize lesions into detailed assessment categories/subcategories (Category 4A, 4B, 4C and 5).

Conclusion: Lesion size is an independent contributor in diagnosing solitary breast masses. Adding the information of lesion size to BI-RADS-MRI 2013 descriptors will allow more detailed categorizations.

Keywords: *breast, magnetic resonance imaging, BI-RADS, mass, size*

Introduction

MRI is recommended in evaluating breast lesion with inconclusive results on mammography and ultrasonography and for diagnosing the extent of breast cancer.[1] The American College of Radiology (ACR) BI-RADS-MRI lexicon, first published in 2003 and revised in 2013 with several alterations in concept and terminology, was developed to standardize interpretation of breast MR images.[2] BI-RADS-MRI descriptors consist of morphology and enhancement/kinetic characteristics. The effectiveness of diagnostic criteria combining morphology and enhancement/kinetic characteristics have been reported,[3–8] but specificity was relatively low with large variation among studies (21–100%).[9] Several interpretation models or decision trees have been proposed.[3,4,6,10] However, the latest version of BI-RADS-MRI does not contain definite criteria for final assessment categories.

Various attempts have been reported to improve diagnostic accuracy, by adding apparent diffusion coefficient (ADC) values or lesion size adjunct to BI-RADS-MRI descriptors.[7,11,12] Yabuuchi et al. and Partridge et al. reported that ADC value as an adjunct to conventional breast MRI (DCE-MRI) improved diagnostic performance.[7,12] Liberman et al. first reported that the frequency of malignancy increases with increasing lesion size,[13] and this was supported by Gutierrez et al., who first described the relevancy of lesion size and BI-RADS-MRI descriptors.[11] They reported that large size (≥1 cm), heterogeneous or rim enhancement,

[1]Department of Diagnostic Imaging and Nuclear Medicine, Kyoto University Graduate School of Medicine, 54 Shogoin-kawaharacho, Sakyo-ku, Kyoto, Kyoto 606-8507, Japan
[2]Department of Breast Surgery, Kyoto University Graduate School of Medicine, Kyoto, Japan
*Corresponding author, Phone: +81-75-751-3760, Fax +81-75-771-9709, E-mail: makok@kuhp.kyoto-u.ac.jp

Received: February 15, 2017 | Accepted: September 14, 2017

irregular or spiculated margins were strongly associated with malignancy in the diagnosis of masses. For benign lesions, in particular fibrocystic changes (FCC), there have been few MR imaging studies;[14] however, some benign lesions, like papilloma, are associated with smaller size,[15] indicating that the pathological background of benign lesions might provide some perspective as to why lesion size is useful in the diagnosis of breast masses. Currently, lesion size is part of a constructed report recommended by BI-RADS-MRI 2013, but its association with likelihood of malignancy is not mentioned.

The purpose of our study was to examine the value of lesion size and ADC value as adjuncts to BI-RADS-MRI 2013 descriptors in diagnostic procedures in determining detailed assessment categories, using a population mainly scanned by a 3.0 Tesla scanner.

Materials and Methods

Study population

This study was approved by our institutional review board and written informed consent was waived because of the retrospective observational study.

Our MRI reporting database, containing 2,603 consecutive MRI reports covering 5 years from April 2008 to March 2013, was retrospectively searched. MRI reports were written as constructed reports according to ACR BI-RADS-MRI 2003 or 2013. The candidate reports were selected from the database using the keyword 'mass'. Exclusion criteria were 1) two or more masses or non-mass enhancement in the same breast 2) post/under-treatment of known breast carcinoma or phyllodes tumor 3) lacking contrast enhanced study, diffusion weighted image, or pathological diagnosis. In total, 250 pathologically confirmed solitary breast masses were included.

The purposes of the MR examination in this study population were 1) lesion characterization of breast masses with indeterminate results on mammography and /or ultrasonography (n = 214), followed by 2) preoperative evaluation of disease extent or additional lesions in ipsi- /contra-lateral breast (n = 36). No high-risk screening MR examination was included in this study.

MRI acquisition

Breast MRI was performed with a 3.0/1.5 Tesla scanner (MAGNETOM Trio/Avanto, A Tim System; Siemens AG, Erlangen, Germany) with a 16/4 channel dedicated breast coil and the patient in the prone position. Out of 250 cases, 206 were performed with a 3.0 Tesla scanner and the remaining 44 cases were performed with a 1.5 Tesla scanner. T_2-weighted, T_1-weighted, diffusion-weighted, fat-suppressed T_1-weighted dynamic contrast-enhanced (DCE) images, and high spatial resolution T_1-weighted contrast-enhanced images were obtained. Detailed acquisition parameters are listed in Table 1. Infused Gadolinium contrast materials were either Gadoteridol (ProHance; Eisai Inc., Tokyo, Japan) or Gadodimide (Omniscan; Daiichisankyo Inc., Tokyo, Japan). The contrast material was intravenously infused at a dose of 0.2 ml/kg and at a rate of 2.0 ml/s, flushed by 20 ml of saline at the same rate.

Image analysis

All of the images were transferred to a Picture Archiving and Communication System (Centricity PACS version 4.0; GE Healthcare integrated IT solutions, Barrington, IL, USA), and size, kinetics and ADC values were evaluated using Aquarius viewer (TeraRecon, Foster City, CA, USA). MRI findings were classified according to the following reporting format, based on BI-RADS-MRI 2013. One radiologist (M. Kawai, with 5 years of experience in breast MRI) re-evaluated all cases according to BI-RADS-MRI 2013 without referring to the original reports. Any difficulties in classification were discussed with another radiologist (M. Iima, with 7 years of experience in breast MRI) to determine the final evaluation.

The maximum diameter of the lesion was measured in high spatial resolution T_1-weighted contrast-enhanced images with multiplanar reconstruction view using Aquarius NET Viewer (TeraRecon). The evaluation criteria included shape, margin, internal enhancing characteristics (IEC) and kinetics, according to BI-RADS-MRI 2013.[2] For margin, lesions were classified as either circumscribed or not-circumscribed (irregular and spiculated were combined as not-circumscribed). For kinetics, the worst looking curve was evaluated within the lesion, as recommended by BI-RADS-MRI 2013. The ADC value of the lesion was evaluated as follows. Circular ROIs of 5 mm in diameter were placed in triplicate on the area of the ADC map visually recognized as the lowest ADC value, carefully avoiding the low signal area in DWI. The minimum ADC value was determined as the lowest mean value within the three circular ROIs.

Inter-observer variability in lesion size were evaluated by comparing size measured by the first observer and the second observer (M. Kataoka, with 17 years of experience in breast MRI). Intra-observer variability in lesion size were evaluated by repeated measurement of the lesion size by the second observer, recorded 2-months after the first measurement. Intra-class correlation coefficient were calculated for both inter-observer and intra-observer variability.

Pathological analysis

All diagnoses were confirmed by pathology (histology or cytology) diagnosed by pathologists with more than ten years of experience in breast pathology. Of the 250 lesions, 157 lesions were obtained by surgical excision, 40 lesions by ultrasound or stereo guided vacuum-assisted biopsy, 27 lesions by core needle biopsy, and 26 lesions by fine needle aspiration. There were four phyllodes tumor cases; two were diagnosed as phyllodes tumor benign, and the other two were diagnosed as phyllodes tumor borderline. In the current analysis, we classified phyllodes tumor benign as 'benign' and phyllodes tumor borderline as 'malignant'.

Table 1. Summary of MRI scanning protocols

Parameter	3.0-T Trio (Siemens) (n = 206)	1.5-T Avant (Siemens) (n = 44)
T_2-weighted images		
Sequence	Axial 2D-turbo spin echo with fat suppression	Axial 2D-turbo spin echo with fat suppression
TR/TE	5500/77	5500/83
Slice thickness (mm)	3	3
Matrix size	448 × 336	448 × 336
FOV (mm)	330 × 330	330 × 330
NEX	1	1
T_1-weighted images		
Sequence	Axial 3D-VIBE	Axial 3D-VIBE
TR/TE	4.83/2.45	7.33/4.76
Slice thickness (mm)	1.5	1.5
Matrix size	448 × 399	448 × 358
FOV (mm)	330 × 330	330 × 330
NEX	1	1
Diffusion-weighted images		
Sequence	Axial single-shot EPI	Axial single-shot EPI
TR/TE	7000/62	9000/78
Slice thickness (mm)	3	3
Matrix size	166 × 80	150 × 72
FOV (mm)	330 × 160	330 × 165
NEX	3	3
b-value (sec/mm^2)	0, 1000	0, 1000
Dynamic study		
Sequence	Axial 3D-VIBE with fat suppression; one precontrast and three contrast-enhanced (at 0–1, 1–2, 5–6 min after gadolinium injection)	Axial 3D-VIBE with fat suppression; one precontrast and three contrast-enhanced (at 0–1, 1–2, 5–6 min after gadolinium injection)
TR/TE	3.70/1.36	4.00/1.43
Flip angle (°)	15	15
Slice thickness (mm)	1	1.5
Matrix size	384 × 346	448 × 336
FOV (mm)	330 × 330	330 × 330
NEX	1	1
High resolution contrast-enhanced T_1 weighted image		
Sequence	Coronal 3D-VIBE with fat suppression; contrast-enhanced (at 2–4.5 min after gadolinium injection)	Coronal 3D-VIBE with fat suppression; contrast-enhanced (at 2–4.5 min after gadolinium injection)
TR/TE	4.01/1.63	4.70/1.73
Flip angle (°)	15	15
Slice thickness (mm)	0.8	0.8
Matrix size	512 × 461	448 × 403
FOV (mm)	330 × 330	330 × 330
NEX	1	1

EPI, echo planar imaging; NEX, number of excitation; VIBE, volumetric interpolated breath-hold examination.

Data analysis

Univariate analysis for lesion size, ADC value, and BI-RADS descriptors were performed. Selection criteria for BI-RADS descriptors to be included in multivariate logistic regression analysis were most frequently seen in malignant masses among several significant descriptors of the same category (shape, margin, IEC and kinetics). To binarize lesion size and ADC value, which are continuous variables, the optimal cut-off value for distinguishing malignant from benign which maximized the Youden index (sensitivity + specificity − 1) in receiver operator characteristic (ROC) analysis was determined. Multivariate analysis was performed to identify parameters that significantly contributed to differentiate malignant from benign, using BI-RADS descriptors, lesion size and ADC value. Results were statistically significant when *P*-value was less than 0.05.

Recursive partitioning analysis was performed to construct a decision tree using significant parameters in multivariate logistic regression analysis. The recursive partitioning was conducted by using the maximized entropy index.[16–19] Decision tree was determined as the best possible model to diagnose malignant masses from benign masses. positive predictive value (PPV) of each node was then calculated and the corresponding BI-RADS categories were allocated. In order to stratify Category 4 in detail, a subcategory system of BI-RADS-Mammography was used: Category 4A, 4B, and 4C with PPV of >2% to ≤10%, >10% to ≤50%, and >50% to <95%, respectively.

Data were entered into a computerized spreadsheet (Excel, Microsoft), and statistical analyses were performed using JMP® 11 (SAS Institute Inc., Cary, NC, USA).

Results

Pathological findings are summarized in Table 2. Of all 250 lesions, 152 lesions (61%) were malignant and 98 lesions (39%) were benign. The frequency of malignancy increased with increasing lesion size up to 20 mm (Fig. 1).

Univariate and multivariate logistic regression analysis

The optimal cut-off value for lesion size was determined to be 12 mm by ROC analysis with a sensitivity of 81.6% and specificity of 50.0%. The optimal cut-off value for ADC value was determined to be 1.1×10^{-3} mm^2/sec by ROC analysis with a sensitivity of 87.5% and specificity of 67.4%.

Regarding lesion size measurement, both inter and intra-observer variability demonstrated high intra-class correlation coefficient (0.993: 95% confidence interval 0.991–0.995, and 0.996: 95% confidence interval 0.995–0.997, respectively.), suggesting that lesion size of solitary breast masses can be a reliable parameter.

Table 2. Pathological findings

Finding	No. of occurrence	Size (mean ± S.D.) (mm)
Malignant	152	25.0 ± 19.1
Invasive carcinoma of no special type	118	25.0 ± 19.2
Invasive lobular carcinoma	9	15.2 ± 6.5
Mucinous carcinoma	5	23.8 ± 13.3
Tubular carcinoma	1	10.0
Cribriform carcinoma	1	19.0
Ductal carcinoma *in situ*	10	20.6 ± 15.6
Lobular carcinoma *in situ*	1	13.0
Malignant lymphoma	2	43.0 ± 26.0
Stromal sarcoma	1	80.0
Malignant peripheral nerve sheath tumor	1	28.0
Chroloma	1	65.0
Phyllodes tumor (borderline)	2	28.5 ± 11.5
Benign	98	17.8 ± 15.7
Fibroadenoma	42	19.9 ± 15.4
Fibrocystic change (FCC)*	22	11.2 ± 5.4
Papilloma	10	11.0 ± 5.4
Inflammatory change	4	23.8 ± 17.2
Hamartoma	3	29.3 ± 5.4
Pseudoangiomatous stromal hyperplasia	3	65.0 ± 24.8
Phyllodes tumor (benign)	2	28.5 ± 7.5
No malignancy	12	9.9 ± 5.0

*including 17 proliferative and 5 non-proliferative FCC.

In order to address potential change of ADC values under different magnetic field strength, ADC values of the 3T dataset (n = 204) and the 1.5T dataset (n = 44) were compared using paired t-test. Overall, the ADC values of the 1.5T dataset (mean ± S.D. $1.1 \pm 0.4 \times 10^{-3}$ mm^2/s) were slightly higher than those of the 3T dataset ($1.0 \pm 0.4 \times 10^{-3}$ mm^2/s). However, the difference was not statistically significant (P = 0.08). Therefore, 3T dataset and 1.5T dataset were analyzed together in the following analysis.

Univariate and multivariate logistic regression analysis of lesion size, ADC value and BI-RADS descriptors are summarized in Table 3. Univariate analysis showed that lesion size, ADC value and most BI-RADS descriptors were significant. ADC value had a smaller P value than lesion size. As more than one feature in each category had P values <0.001 in the univariate logistic regression analysis, we chose the most frequently seen significant features for malignancy to avoid collinearity problems in the multiple regression analysis.

Multivariate logistic regression analysis was performed using lesion size (≥ 12 mm or not), ADC value (< 1.1 × 10^{-3} mm^2/s or not), shape (irregular or not), margin (circumscribed or not-circumscribed), IEC (rim enhancement present or absent), and kinetics (washout or not). Margin, lesion size, kinetics, and IEC were significant parameters ($P < 0.05$) for diagnosing malignant masses. ADC value and shape were not significant.

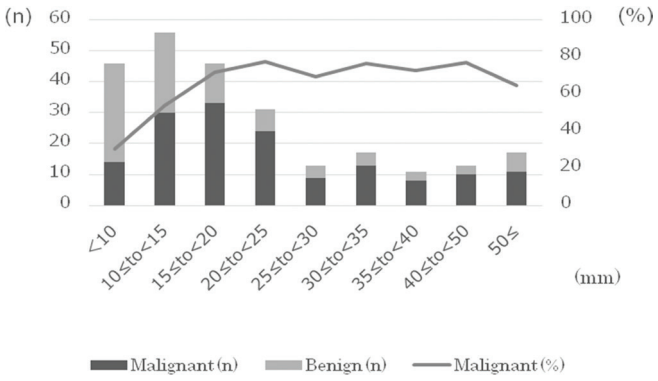

Fig. 1 Lesion size and frequency of malignancy. The box plot indicates the number of malignant and benign lesions classified according to lesion size. The line graph indicates the percentage of malignant lesions. The horizontal axis corresponds to lesion size (mm), the left vertical axis corresponds to number of cases and the right axis corresponds to percentage.

Decision tree

Using the four parameters found to be significant by multivariate logistic regression analysis, a decision tree was constructed as the best possible model to diagnose malignant from benign masses (Fig. 2). A total of 250 cases were first divided into two by margin (circumscribed or not-circumscribed) (first node). Secondly, the not-circumscribed group was divided by IEC (rim enhancement present or absent) (second node), while the circumscribed group was divided by kinetics (washout or not) (second node). Then, the 'not-circumscribed and rim enhancement' and 'circumscribed and washout' groups were further divided by lesion size (<12 mm or ≥12 mm) (third node). Without the third node of lesion size, there were only two categories, Category 4A and Category 4C. With the third node of lesion size added, however, the 'not-circumscribed and rim enhancement' group was divided into Category 4C and Category 5, and the 'circumscribed and washout' group was divided into Category 4B and Category 4C. In this decision tree, lesion size contributed in risk

Table 3. Results of univariate and multivariate logistic regression analysis

Feature	Malignant (%) n = 152	Benign (%) n = 98	Univariate logistic regression analysis	Multivariate logistic regression analysis		
			P value	Odds ratio	95% CI	P value
Size (mean ± S.D.) (mm)	25.0 ± 19.1	17.8 ± 15.7	0.001*	3.99	1.7–9.7	0.001*
ADC value (mean ± S.D.) (×10^{-3} mm^2/s)	0.85 ± 0.26	1.26 ± 0.38	<0.001*	2.35	0.95–5.8	0.065
Shape						
Round	35 (23.0)	20 (20.4)	0.626			
Oval	28 (18.4)	65 (66.3)	<0.001*			
Irregular	89 (58.5)	13 (13.3)	<0.001*,†	1.31	0.45–3.8	0.613
Margin						
Circumscribed	24 (15.8)	76 (77.6)	<0.001*			
Not-circumscribed	128 (84.2)	22 (22.5)	<0.001*,†	7.15	2.9–18.5	<0.001*
Internal enhancement						
Homogeneous	3 (2.0)	22 (22.4)	<0.001*			
Heterogeneous	32 (21.1)	44 (44.9)	<0.001*			
Rim enhancement	116 (76.3)	16 (16.3)	<0.001*,†	3.46	1.3–9.1	0.012*
Dark internal septations	1 (0.7)	16 (16.3)	0.001*			
Kinetics						
Persistent	6 (3.9)	49 (50.0)	<0.001*			
Plateau	11 (7.2)	20 (20.4)	0.003*			
Washout	135 (88.8)	29 (29.6)	0.001*,†	3.71	1.4–9.8	0.008*

ADC, apparent diffusion coefficient; CI, confidence interval; *, Factors statistically significant ($P < 0.05$); †, Most frequent descriptors per each category, selected for the multiple regression analysis.

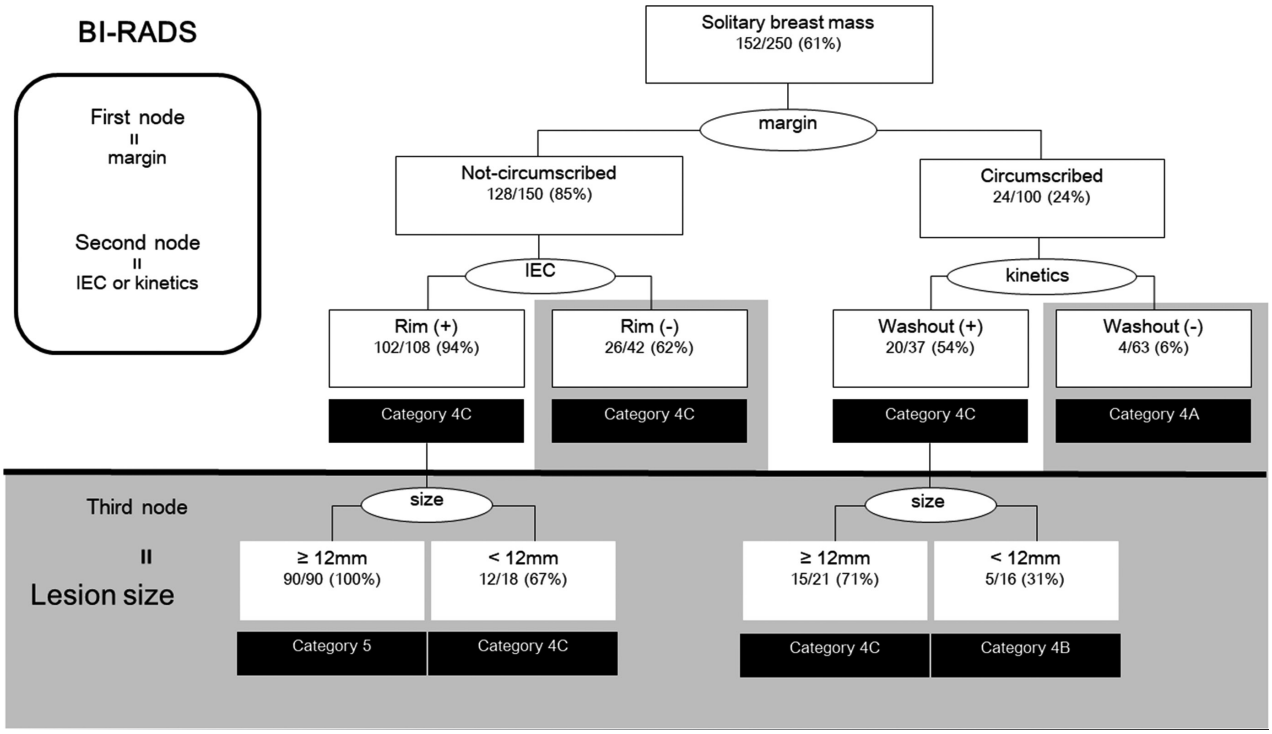

Fig. 2 Proposed decision tree. Positive predictive value (PPV) is shown in parentheses. In BI-RADS-MRI, Categories 1, 2, 3, 4, and 5 are determined with a PPV of 0%, 0%, >0% to ≤2%, >2% to ≤95%, and ≥95% to ≤100%, respectively. Category 4 is subcategorized as Category 4A, 4B, and 4C, with PPVs of >2% to ≤10%, >10% to ≤50%, and >50% to <95%, respectively, similar to the subcategory system of BI-RADS-Mammography. The 250 cases were classified into two categories by BI-RADS (above bar), and then into four categories by adding lesion size (gray shadow).

stratification of two groups, the 'not-circumscribed and rim enhancement' group and the 'circumscribed and washout' group. Representative cases of solitary masses with similar BI-RADS descriptors and different size categories are shown in Fig. 3.

Discussion

In our study, lesion size was significant in diagnosing malignant solitary breast masses in both univariate and multivariate logistic regression analyses. Lesion size was significant in multivariate logistic regression analysis, whereas ADC value was not significant, indicating that lesion size is a parameter that is relatively independent of the BI-RADS-MRI 2013 descriptors. Also lesion size seemed to be a reliable quantifiable variables with high inter- and intra-observer reliability.

There are a limited number of previous studies examining both lesion size and BI-RADS descriptors. Yabuuchi et al. have investigated mass cases and reported that lesion size was not significant in univariate logistic regression analysis.[7] Gutierrez et al. reported that lesion size was significant in univariate logistic regression analysis for mass, but not for non-mass enhancement or focus.[11] In our solitary mass study, lesion size was significant in both univariate and multivariate logistic regression analyses. These conflicting results might be attributable to the difference in the prevalence of breast cancer; 84%[7] and 32%[11] in the previous studies compared with 61% in our study. The prevalence of breast cancer and lesion size distribution may be affected by the purpose of MR examination; problem-solving, preoperative evaluation, or screening. The purpose of MR examination in our study is predominantly for lesion characterization and problem solving. Due to difference in prevalence of breast cancer and size distributions, our proposed decision tree may not be applicable to the different patient populations.

Lesion size was an independent and significant contributor in diagnosis when combined with other selected BI-RADS descriptors. This can be explained by the association of size distribution and pathological background. Pathologically, some benign lesions are considered to be size limiting. For example, most intraductal papillomas are smaller than 5 mm in diameter.[15] In studies using breast MRI, intraductal papillomas were frequently less than 20 mm.[20,21] FCCs in our study are relatively small in size. FCC can be large, but typically present as a non-mass enhancement.[14] Some of FCCs in our study were presented as focal lesions that are known to mimic breast cancer due to their washout kinetics.[22]

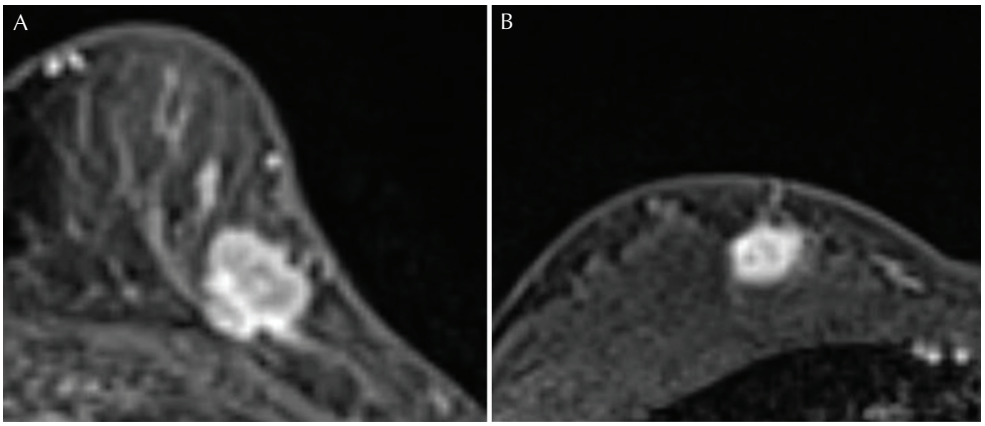

Fig. 3 A 71-year old woman with invasive ductal carcinoma of no special type, 15 mm in diameter (**A**: left) and 18 year-old woman with intraductal papilloma, 11 mm in diameter (**B**: right). Axial T_1-weighted dynamic contrast-enhanced images in the delayed phase. Each image show a mass with not-circumscribed margin, rim enhancement, and fast/washout kinetics. Both lesions look similar in shape, margin and internal enhancement pattern. In such context, lesion size might help to make the correct categorization. According to the proposed decision tree, the lesion in panel (**A**) is classified as Category 5, while the lesion in panel (**B**) is classified as Category 4C with up to 50% possibility of benign lesion.

Our proposed decision tree effectively classified breast masses into detailed assessment categories, which may lead to appropriate management. In this decision tree, lesions are first classified using BI-RADS mass descriptors, followed by lesion size, which is straightforward and easy to comprehend. The proposed decision tree follows the concepts of previous decision tree models,[3,4,6] combining margin, IEC and kinetics. Our idea is that adding lesion size to the former proposed interpretation models might be useful. Measurement of lesion size is a conventional approach that does not require extra MR imaging, and thus would be beneficial to all radiologists in general hospitals.

MRI techniques and the capabilities of MR scanners have improved greatly in the last decade, and usage of the 3.0T has become more common. Our study might provide some insights on the clinical applications of BI-RADS-MRI 2013 with improved image quality. Category 4 varies in percentage of malignant risk, from 2% to 95%. A recent study by Maltez de Almeida et al. reported that category 4 subcategorization can be satisfactorily performed with DCE-MRI.[23] Our results are in line with their conclusions. Currently, BI-RADS-mammography advocates the use of subcategories, because detailed subcategorization/risk stratification will allow for a more meaningful practice audit, will be useful in research involving ROC curve analysis, and will be an aid for clinicians and pathologists.[2] The scientific literature on MRI, unlike mammography, is not sufficient to indicate specific cut-off points for the subdivisions of Category 4 assessments.[2] Nevertheless the results of the current study might help to establish such cut-off points. Studies including a larger number of cases and different populations, including Category 4 subdivisions, will be required to further develop BI-RADS-MRI.

Our study has some limitations. First, it was a retrospective single site study. Our results including decision tree will need to be validated in a future prospective study with a different dataset. Second, the inclusion criteria of pathology-proven cases excluded many small benign lesions, which may have introduced sampling bias.

Conclusion

Lesion size is an independent contributor in diagnosing solitary breast masses. A decision tree using lesion size combined with BI-RADS-MRI 2013 descriptors will allow more detailed categorizations.

Conflicts of Interests

The authors declare that there is no conflict of interest.

References

1. Tozaki M, Isomoto I, Kojima Y, et al. The Japanese Breast Cancer Society Clinical Practice Guideline for screening and imaging diagnosis of breast cancer. Breast Cancer 2015; 22:28–36.
2. Morris EA, Comstock CE, Lee CH, et al. ACR BI-RADS® Magnetic Resonance Imaging. In: ACR BI-RADS® Atlas, Breast Imaging Reporting and Data System. Reston, VA: American College of Radiology; 2013.
3. Kinkel K, Helbich TH, Esserman LJ, et al. Dynamic high-spatial-resolution MR imaging of suspicious breast lesions: diagnostic criteria and interobserver variability. AJR Am J Roentgenol 2000; 175:35–43.
4. Nunes LW, Schnall MD, Orel SG. Update of breast MR imaging architectural interpretation model. Radiology 2001; 219:484–494.

5. Szabó BK, Aspelin P, Wiberg MK, Boné B. Dynamic MR imaging of the breast. Analysis of kinetic and morphologic diagnostic criteria. Acta radiologica 2003; 44:379–386.
6. Tozaki M, Igarashi T, Matsushima S, Fukuda K. High-spatial-resolution MR imaging of focal breast masses: interpretation model based on kinetic and morphological parameters. Radiat Med 2005; 23:43–50.
7. Yabuuchi H, Matsuo Y, Okafuji T, et al. Enhanced mass on contrast-enhanced breast MR imaging: Lesion characterization using combination of dynamic contrast-enhanced and diffusion-weighted MR images. J Magn Reson Imaging 2008; 28:1157–1165.
8. Goto M, Ito H, Akazawa K, et al. Diagnosis of breast tumors by contrast-enhanced MR imaging: comparison between the diagnostic performance of dynamic enhancement patterns and morphologic features. J Magn Reson Imaging 2007; 25:104–112.
9. Kuhl CK. Current status of breast MR imaging. Part 2. Clinical applications. Radiology 2007; 244:672–691.
10. Schnall MD, Blume J, Bluemke DA, et al. Diagnostic architectural and dynamic features at breast MR imaging: multicenter study. Radiology 2006; 238:42–53.
11. Gutierrez RL, DeMartini WB, Eby PR, Kurland BF, Peacock S, Lehman CD. BI-RADS lesion characteristics predict likelihood of malignancy in breast MRI for masses but not for nonmasslike enhancement. AJR Am J Roentgenol 2009; 193:994–1000.
12. Partridge SC, DeMartini WB, Kurland BF, Eby PR, White SW, Lehman CD. Quantitative diffusion-weighted imaging as an adjunct to conventional breast MRI for improved positive predictive value. AJR Am J Roentgenol 2009; 193:1716–1722.
13. Liberman L, Mason G, Morris EA, Dershaw DD. Does size matter? Positive predictive value of MRI-detected breast lesions as a function of lesion size. AJR Am J Roentgenol 2006; 186:426–430.
14. van den Bosch MA, Daniel BL, Mariano MN, et al. Magnetic resonance imaging characteristics of fibrocystic change of the breast. Invest Radiol 2005; 40:436–441.
15. Daniel BL, Gardner RW, Birdwell RL, Nowels KW, Johnson D. Magnetic resonance imaging of intraductal papilloma of the breast. Magn Reson Imaging 2003; 21:887–892.
16. JMP® 10 Modeling and Multivariate Methods. In. Cary, NC, USA: SAS Institute Inc., 2012. https://support.sas.com/documentation/onlinedoc/jmp/10/Modeling_Multivariate.pdf (Accessed July 20, 2017).
17. James KE, White RF, Kraemer HC. Repeated split sample validation to assess logistic regression and recursive partitioning: an application to the prediction of cognitive impairment. Stat Med 2005; 24:3019–3035.
18. Abe T, Tokuda Y, Cook EF. Time-based partitioning model for predicting neurologically favorable outcome among adults with witnessed bystander out-of-hospital CPA. PLoS ONE 2011; 6:e28581.
19. Goto Y, Maeda T, Goto Y. Decision-tree model for predicting outcomes after out-of-hospital cardiac arrest in the emergency department. Crit Care 2013; 17:R133. doi: 10.1186/cc12812.
20. Tominaga J, Hama H, Kimura N, Takahashi S. Magnetic resonance imaging of intraductal papillomas of the breast. J Comput Assist Tomogr 2011; 35:153–157.
21. Zhu Y, Zhang S, Liu P, Lu H, Xu Y, Yang WT. Solitary intraductal papillomas of the breast: MRI features and differentiation from small invasive ductal carcinomas. AJR Am J Roentgenol 2012; 199:936–942.
22. Chen JH, Nalcioglu O, Su MY. Fibrocystic change of the breast presenting as a focal lesion mimicking breast cancer in MR imaging. J Magn Reson Imaging 2008; 28:1499–1505.
23. Maltez de Almeida JR, Gomes AB, Barros TP, Fahel PE, de Seixas Rocha M. Subcategorization of suspicious breast lesions (bi-rads category 4) according to MRI criteria: role of dynamic contrast-enhanced and diffusion-weighted imaging. AJR Am J Roentgenol 2015; 205:222–231.